J MATER RES TECHNOL. 2020;xxx(xx):xxx–xxx

Available online at www.sciencedirect.com

jmr&t Journal of Materials Research and Technology

www.jmrt.com.br

Original Article

Elimination of edge cracks and centerline segregation of twin-roll cast aluminum strip by ultrasonic melt treatment

Jinxian Huang[a], *Jianguo Li*[a,*], *Cong Li*[b], *Chunfa Huang*[a], *Bernd Friedrich*[b]

[a] *School of Materials Science and Engineering, Tsinghua University, 100084 Beijing, China*
[b] *IME Institute of Process Metallurgy and Metal Recycling, RWTH Aachen University, 52056 Aachen, Germany*

ARTICLE INFO

Article history:
Received 24 September 2019
Accepted 6 March 2020
Available online xxx

Keywords:
Edge cracks
Centerline segregation
Ultrasonic
Twin-roll casting
Iron intermetallic

ABSTRACT

Ultrasonic-assisted twin-roll casting (UA-TRC) process was developed for the production of high quality 1050 aluminum alloy strip with minimum casting defects. Results of industrial-scale trials show that the strips obtained by UA-TRC exhibited a homogenized matrix composed of fine equiaxed grains. Meanwhile, robust evidence substantiates the feasibility of eliminating edge cracks and centerline segregation of the strips via the ultrasonic melt treatment. Scanning electron microscopy (SEM) and electron backscatter diffraction (EBSD) techniques were utilized to clarify the cause of edge cracks and centerline segregation, and furthermore, the regime of elimination of such defects via ultrasonic treatment in TRC processing. The results of present study reveal that by introduction of ultrasonic prior to rolling, homogeneity of solute elements and fluidity of the melt can be enhanced. As a result, the production of non-cracked strips with homogenized matrix is promised.

1. Introduction

Twin-roll casting (TRC) has been developed in industrial plants over three decades [1–3]. Unlike the conventional way of producing strips by rolling billets, this continuous strip casting process method provides an attractive convenience of directly converting the liquid metal to solid strips. Owning to flexibility and relatively low production cost, this process has been widely used in aluminum industries. In production, the aluminum melt from the furnace is firstly transferred to the headbox through the launder system and fed subsequently to the gap of two water-cooled rolls by a refractory feed nozzle, where it undergoes a rapid solidification and hot deformation before finally forming a gauge solid strip.

Commercial grain refiner (e.g., Al-5Ti-1B) is beneficial for the TRC processing. TiB_2 particles inoculated into melt through Al-5Ti-B master alloys are able to enhance heterogeneous nucleation of α-Al grains. However, the inoculant particles introduced are seen as undesired inclusions in downstream processing of ingots and many defects still occur [4]. The quality of strips is always a concern because most casting defects are hardly controlled by the subsequent rolling and heat treatment processes. The defects of strips produced by TRC are divided into two types, surface defects and internal defects. Surface defects such as level lines, streakings, and cracks can be readily observed by naked eye, whereas the inter-

* *Corresponding author.*
E-mail: jg.li@mail.tsinghua.edu.cn (J. Li).
https://doi.org/10.1016/j.jmrt.2020.03.021

Please cite this article in press as: Huang J, et al. Elimination of edge cracks and centerline segregation of twin-roll cast aluminum strip by ultrasonic melt treatment. J Mater Res Technol. 2020. https://doi.org/10.1016/j.jmrt.2020.03.021

nal defects e.g., centerline segregation [5], inhomogeneous microstructure, underlying voids, and nonmetallic inclusions are hard to detect in industrial production. One of the most problematic issues in the TRC production is edge crack, which leads to not only unsatisfied product appearance but also difficulties in processing of strips at downstream [6]. Centerline segregation, namely severe segregation of solute elements in the center of the strips, is a typical internal defect occurs during TRC process, which appears in the final solidified zone of the as-cast strip. This kind of defect adversely influences the homogeneity of composition and mechanical properties, decreasing the fatigue strength, leads to local microcracks and porosities [7]. Eliminating centerline segregation in TRC aluminum strips by changing rolling parameters have been studied over decades [8]. However, when rolling parameters were adjusted, the productivity was often affected as well. Therefore, controlling centerline segregation during the TRC process is a formidable challenge [9].

In order to minimize the defects of strips, a handful of technologies have been developed in recent years. Barekar et al. [10,11] and Kim [12] exploited liquid melt-conditioning twin-roll casting (MC-TRC) technology to control centerline segregation, during which an intensive shearing apparatus in the tundish was employed to dispersed heterogeneous nucleation substrates throughout the whole volume to controlled the solidification of the liquid metal. Electromagnetic field-assisted technology is another one that found to be relatively effective in alleviating the centerline segregation in TRC processing [13]. In practice, non-cracked strips can be realized with special adjustments such as the shape of the feed nozzle, casting speed, etc. However, few of those technologies are capable of eliminating edge cracks and centerline segregation simultaneously. Therefore, a general technique for producing high-quality TRC strips is in urgent need. One of the most potential solutions is offered by ultrasonic-assisted process.

Ultrasonic assisted technology is a promising technique in the aluminum industry and a substantial amount of fundamental and practical work has been conducted on that. Upon propagation, ultrasonic waves in aluminum melt give rise to two phenomena simultaneously, cavitation and acoustic streaming. The cavitation is a process involving the formation, growth, pulsating and implosive collapse of tiny bubbles in the melt. The rapid collapsing of these unstable bubbles generates locally high temperature and pressure. Meanwhile, on account of the absorption of acoustic waves during its propagation in the liquid metal, the quasi-steady liquid flow called acoustic streaming induces an energy gradient throughout the volume. Substantiated effects of acoustic flows in liquid melt are homogenization and intensive melt mixing [14,15], both of which are considered to be great advantages for enhancing the conventional TRC process. Notwithstanding considerable attention has been attracted by ultrasonic energy field technology [16,17], the application of ultrasonic treatment in TRC process has barely been reported. The reasons lie not only in corrosion of sonotrode by aluminum melt at long service time [18,19], but also in lack of fundamental understanding about mechanism of ultrasonic treatment of aluminum melt in industries.

In the present study, the ultrasonic-assisted technology was applied in the TRC processing, with the aim of investigating the effect of ultrasonic field on elimination of edge cracks and centerline segregation. Based on macroscopic observation and microstructure analysis upon strips produced by conventional TRC and UA-TRC process, the grain refinement mechanism and solidification behavior under ultrasonic field were discussed. The comparison between strips produced by conventional TRC and UA-TRC strips demonstrated the advantages and potentials of UA-TRC.

Table 1 – The nominal composition of AA1050 aluminum.

	Alloy Composition Limits, wt. %					
Element	Fe	Si	Cu	Mn	Mg	Al
Content	0.40	0.25	0.05	0.03	0.03	Bal.

Table 2 – The key processing parameters of experiment.

Parameter	Value
Furnace temperature	730 °C
Headbox temperature	690 °C
Casting speed	830 mm/min
Cooling-water flow rate	160 L/min

2. Experimental materials and processes

AA1050 aluminum (99.5 wt.% purity), a widely used material in TRC, was selected for the current research work and the chemical composition is shown in Table 1. A tilting industrial-scale type twin-roll caster consists of two stainless-steel rolls in a diameter of 500 mm and a width of 1300 mm was used to produce strips. The rolls of caster were internally water-cooled and tilted a 75° angle with respect to the horizontal line. The ultrasonic treatment was implemented with different sonotrodes (titanium and niobium, 40 mm in diameter) driven by a piezoelectric ultrasonic water-cooled transducer, which was set at a frequency of 16.5 kHz. The ultrasonic generator provided a maximum 1000 W power for the whole system. The amplitude of vibrations was 20 μm measured in air on an ultrasonic horn using a contactless vibrometer. During the UA-TRC trials, the sonotrode was immersed in a depth of approximately 20 mm below the surface of liquid metal in the headbox and no grain refiner was added. In the conventional TRC trial, an 0.3 wt.% addition of Al-5Ti-1B grain refiner was introduced but yet no ultrasonic treatment was applied. The temperature of the headbox was kept constant at 690 °C, and other process parameters such as casting speed were invariable in all experiments, as specified in Table 2. The dimension of the TRC strip is 1160 mm (width) × 6.8 mm (thickness). In order to testify UA-TRC process's ability to work continuously as well as results reproducibility, the time period of each trial was set at 5 h.

The surface quality of strips namely edge cracks and other surface defects were firstly checked by naked eyes. All specimens used for microstructure characterization were cut in the dimension of 20 × 20 × 6.8 mm from the edge and center of strips, respectively. Afterward they were ground, mechanically polished, electropolished and anodized. The anodization

Please cite this article in press as: Huang J, et al. Elimination of edge cracks and centerline segregation of twin-roll cast aluminum strip by ultrasonic melt treatment. J Mater Res Technol. 2020. https://doi.org/10.1016/j.jmrt.2020.03.021

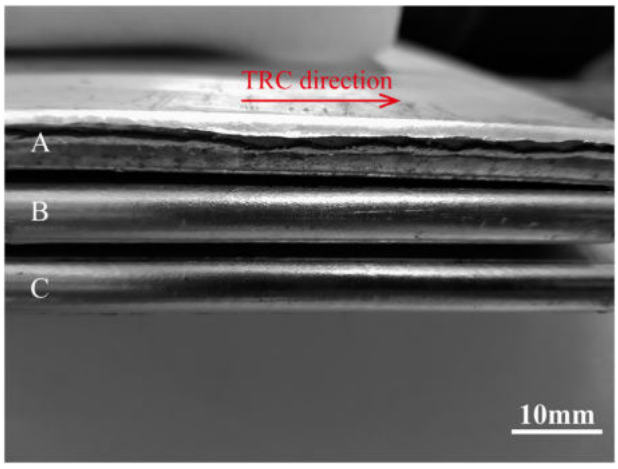

Fig. 1 – The profile of the strips: A: the conventional TRC, B: UA-TRC (titanium) and C: UA-TRC (niobium).

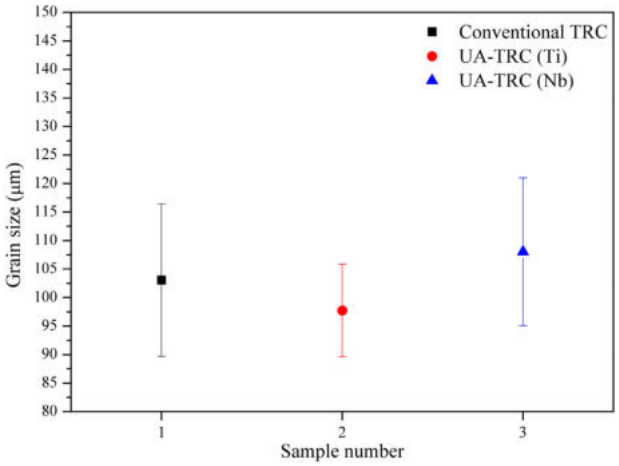

Fig. 3 – The grain size of different TRC strips.

was performed at 20 VDC using Barker's reagent to reveal the grain size distribution.

The grain structure was examined with an optical microscope (Axio Scope-A1) incorporated with polarized light mode and bright field mode, upon the cross (vertical to rolling direction) and longitudinal (along to rolling direction) sections of strips. The linear intercept method was used to measure the average grain size. The composition was analyzed by spark spectrometer (MAX Spectro). Scanning Electron Microscopy (SEM) (FEI Quanta 200FEG) with integrated Flat-Quad Energy Dispersive X-ray spectrum analysis (EDS) was employed to observe the morphology of the edge cracks and determine the intermetallic particles. Further analysis upon the crystal orientation and the strain of grains were characterized by the Electron Backscatter Diffraction (EBSD).

3. Results

3.1. *Edge cracks*

Fig. 1 shows the profile of the strips manufactured by the conventional TRC and UA-TRC. It can be seen clearly a macro-crack emerged in the edge of conventional TRC strip and extended along the TRC direction. However, no visible crack was observed in the UA-TRC strips regardless of sonotrode materials. This observation preliminarily attests that the ultrasonic treatment can eliminate the edge cracks in the TRC processing, which will be a great advantage for the downstream processing.

3.2. *Grain structures*

The grain structure of cross-sections of the edge area in different strips are shown in Fig. 2 In the vicinity of edge crack (Fig. 2(a)), there were a number of equiaxed grains and no obvious coarse dendrite structure was found. Some elongated grains can be found in the area away from the edge crack tip as a result of the deformation during processing. Compared with the conventional TRC strip, an equiaxed grain structure was also exhibited in UA-TRC strips, as displayed in Fig. 2(b) and (c). The average grain size for the edge region of conventional TRC strip, UA-TRC (titanium sonotrode) strip and UA-TRC strip (niobium sonotrode) were 104 μm, 98 μm, and 108 μm, respectively. Given the fact that the values of grain sizes are the same within the experimental error (shown in Fig. 3), it is suggested that a grain refinement can be achieved as comparable as the addition of Al-5Ti-1B grain refiner when the ultrasonic was introduced into the TRC processing.

3.3. *Centerline segregation*

To examine the centerline segregation, the microstructure of the longitudinal sections and cross-sections of the center region of strips (The observed positions in the present study were divided into the edge region and the middle region. For centerline segregation observation, generally, the mid-

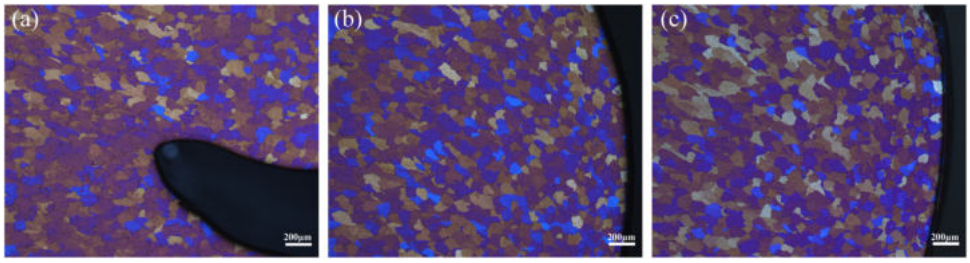

Fig. 2 – Micrographs show the grains distribution of cross sections of the edge region of strips: (a) in the conventional TRC strip, (b) and (c) UA-TRC by titanium sonotrode and niobium sonotrode, respectively.

Please cite this article in press as: Huang J, et al. Elimination of edge cracks and centerline segregation of twin-roll cast aluminum strip by ultrasonic melt treatment. J Mater Res Technol. 2020. https://doi.org/10.1016/j.jmrt.2020.03.021

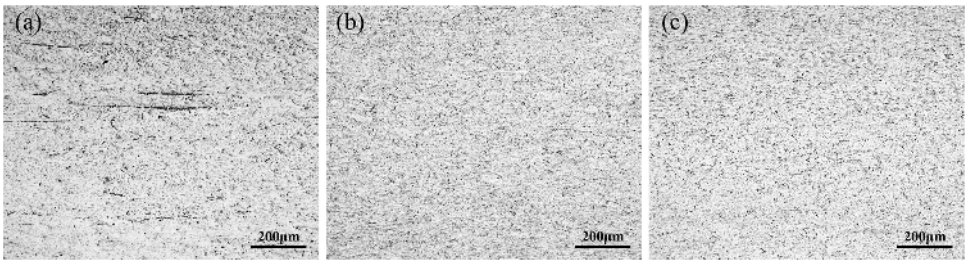

Fig. 4 – Micrographs of the longitudinal sections of the center region of strips: (a) conventional TRC, (b) and (c) UA-TRC by titanium sonotrode and niobium sonotrode, respectively.

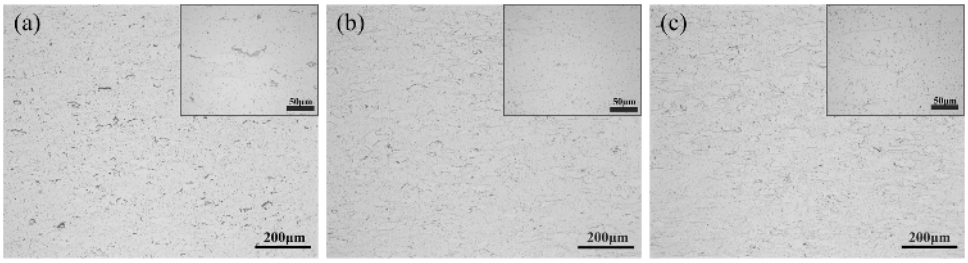

Fig. 5 – Microstructures of the cross sections of the middle region of strips: (a) the conventional TRC, (b) and (c) UA-TRC by titanium sonotrode and niobium sonotrode, respectively. Insets show enlarged image for each strip.

dle region was chosen.) were shown in Figs. 4 and 5. A few black sticks were observed in Fig. 4(a) in the longitudinal section of the conventional TRC strip, which were defined as intermetallics formed due to the centerline segregation. It is believed that the large intermetallics will deteriorate the mechanical properties of aluminum products because of its brittleness. In contrast, UA-TRC strips presented little segregation structure, as is shown in Fig. 4(b) and (c).

In the cross-section of conventional TRC strip (Fig. 5(a)), a number of coarse Fe-rich phases emerged in the middle region, which indicates severe solute segregation in the solidification of the conventional TRC process. Compared to conventional TRC, few coarse Fe-rich phases appeared in the cross-sections of UA-TRC strips in the center region, which suggests that solute segregation was relieved substantially. Based on evidence found in Figs. 4 and 5, it is verified that ultrasonic treatment, when applied in the TRC processing is able to effectively suppress the micro-segregation at the inter-grains region.

3.4. *Morphology of crack surface*

Fig. 6 shows the morphology of the crack surface. A bumpy morphology and the dendrite structure can be clearly observed from the fractography. In Fig. 6(a), a dendrite arm was found to extrude from the surface. No visible cleavage plane and distinct dimple were found in the surface throughout the edge crack, which indicates that such crack is not formed after solidification, instead, it was formed when interdendritic solidification induced shrinkage and the remained liquid flowed by [20]. Even after undergoing a rolling deformation procedure, the crack remained in the final product due to its huge width so that it can be observed by naked eyes. It should be noted that the extruded dendrite arm was found to be covered by an intermetallic, as shown in Fig. 6(b). The intermetallic seems a vine intertwined upon the dendrite and is believed to impede further growth of the dendrite. A closer look of the intermetallic is given in Fig. 7. The EDS pattern unveils that this intermetallic was a Fe-rich phase. Taken the Fe concentration and the cooling rate of TRC processing into account, this intermetallic was a metastable Al-Fe phase, possibly Al_6Fe [21].

3.5. *Microstructure and strain level*

The EBSD technology was used to analyze the microstructure and evaluating the level of strain. The grain size, grain orientation and strain distribution of the conventional TRC and UA-TRC strips were compared in Fig. 8. As seen in Fig. 8(a), inverse pole figure (IPF) indicates that the conventional TRC strip exhibited elongated grains along the crack with a grain size calculated by EBSD software of around 56 μm. The grain size of UA-TRC strip was around 54 μm, as is shown in Fig. 8(b). It seems that both strips have congruent grain size in the edge region. A similar conclusion was also found in Fig. 8(e). Both strips are randomly distributed in grain orientation according to the IPF. The grain boundaries were characterized by low angle grain boundaries (LAGBs; 5°–15°) in red lines, high angle grain boundaries (HAGBs; >15°) in black lines. As it can be seen in Fig. 8(c) and (d), the conventional TRC strip shows a higher fraction of LAGBs than UA-TRC strip, which is a clear indication that the UA-TRC strip underwent a lower strain [22]. Moreover, the conventional strip exhibited a high fraction of LAGBs at the periphery of crack, indicating that strain was concentrated on this region, some grains around the edge of crack had a larger misorientation whilst some others scarcely did. In comparison, the UA-TRC strip at a similar area exhibited a more homogeneous strain pattern, as shown in Fig. 8(d). The

Please cite this article in press as: Huang J, et al. Elimination of edge cracks and centerline segregation of twin-roll cast aluminum strip by ultrasonic melt treatment. J Mater Res Technol. 2020. https://doi.org/10.1016/j.jmrt.2020.03.021

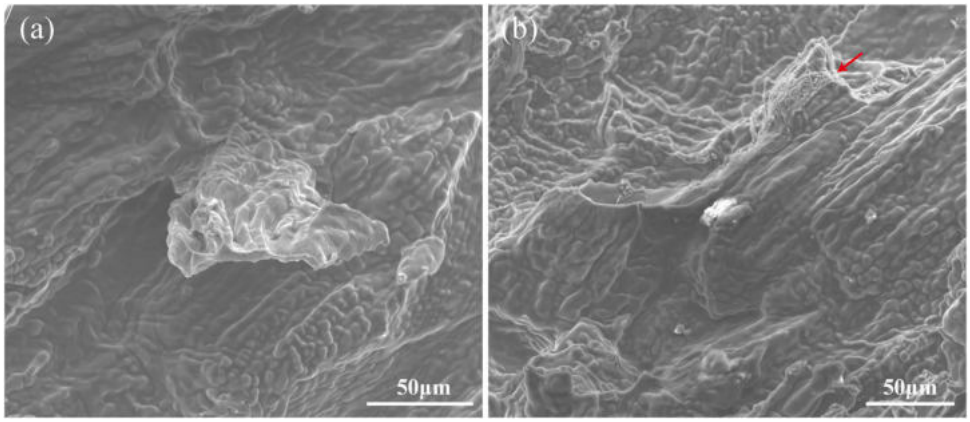

Fig. 6 – Morphology of the edge crack surface in the conventional TRC strips: (a) a dendrite arm extruded from surface, (b) intermetallic (red arrow) upon the dendrite.

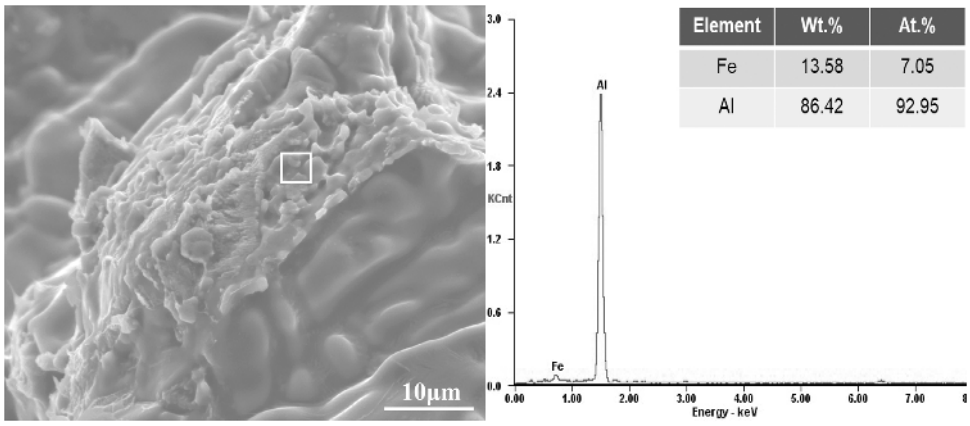

Element	Wt.%	At.%
Fe	13.58	7.05
Al	86.42	92.95

Fig. 7 – A closer view of the intermetallic and the EDS result corresponding to white-square area.

Kernel Average Misorientation (KAM) distribution is shown in Fig. 8(f), the intra-grain misorientation of conventional TRC strip was relatively scattered, while the distribution of UA-TRC narrowed and shifted to some extent towards a lower misorientation. Based on the above results, it seemingly suggested that the UA-TRC strip probably underwent a relatively uniform strain during the processing. However, taken the little difference of KAM values into account, it would not be the main reason for the elimination of edge cracks and still more statistics are needed to support such a conclusion.

3.6. *Feasibility of UA-TRC*

For the sake of examining the feasibility and reproducibility of UA-TRC applying in industrial scale. All UA-TRC experiments either by titanium sonotrode or niobium sonotrode were conducted 5 h continuously. The edge-crack had not occurred throughout, which showing good reproducibility and the feasibility of UA-TRC. As is shown in Fig. 9, there was obvious corrosion at the radiating surface of titanium sonotrode. In contrast, niobium sonotrode had higher corrosion resistance to the liquid aluminum with high temperatures. For the further application of UA-TRC, niobium seems to be a preferable material for sonotrode owing to excellent corrosion resistance.

4. Discussion

4.1. *Mechanism of grain refinement by UA-TRC*

The propagation of ultrasonic waves often induces a whole range of non-linear effects, including cavitation, sonocapillary effect, acoustic streaming, etc. Among all the phenomena associated with the ultrasonic waves through the liquid melt, cavitation is probably the most important one. Microcavities termed “cavitation bubbles” are produced in the liquid melt when the acoustic intensity exceeds the cavitation threshold (80 W/cm^2 in molten aluminum [23]). The acoustic intensity I is given by:

$$I = \frac{1}{2}\rho c(2\pi f A)^2 \quad (1)$$

In which ρ is the density of liquid aluminum (2375 kg/m^3), c is the speed of sound (4725 m/s [16]), f is the frequency (16.5 kHz) and A is the amplitude (20 μm). By substitution these values into Eq. (1), the acoustic intensity in present study was estimated as 2412 W/cm^2, which is much greater than the cavitation threshold required to produce cavitation in liquid aluminum. Hence, bubbles will grow during the negative pressure portion of the sound propagating and finally collapse in

Please cite this article in press as: Huang J, et al. Elimination of edge cracks and centerline segregation of twin-roll cast aluminum strip by ultrasonic melt treatment. J Mater Res Technol. 2020. https://doi.org/10.1016/j.jmrt.2020.03.021

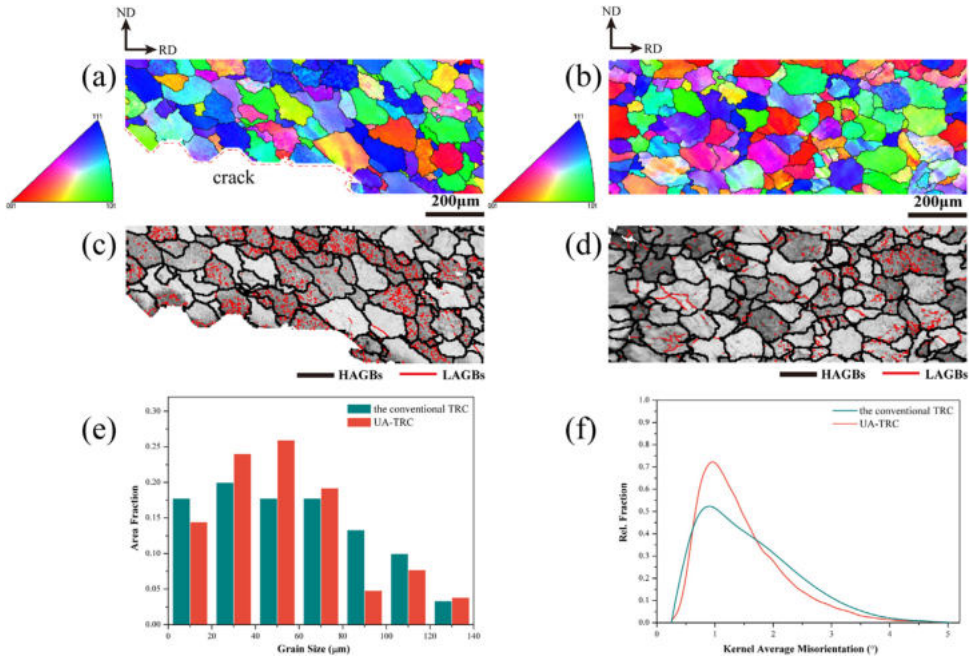

Fig. 8 – Inverse pole figure (IPF), grain boundaries distribution of the edge region of strips: (a) and (c) the conventional TRC, (b) and (d) UA-TRC (titanium), (e) and (f) a comparison of grain size and Kernel Average Misorientation (KAM) distribution, respectively.

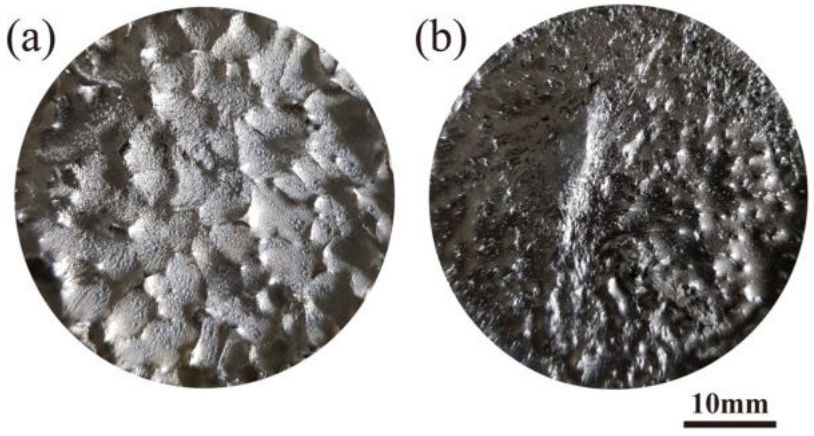

Fig. 9 – Cavitation corrosion of sonotrodes: (a) titanium sonotrode, (b) niobium sonotrode.

the positive portion. It is well known that the collapse occurs in a way of bubbles implosion, which generates instantaneously local high-temperature (roughly 5000 K) and high-pressure (up to in a range of GPa) in liquid melt [24]. Base on the above effects, when ultrasonic waves are introduced to the melt, the possible mechanism of grain refinement can be outlined as follows:

1) The cavitation induced the fragmentation of dendrites during solidification, and these tiny crystals subsequently were transferred by acoustic streaming to other regions where further growth took place. Ultimately, grain refinement is achieved because of the grain nuclei multiplication [25].
2) According to the Clausius–Clapeyron equation, the local high-pressure will increase the theoretical melting temperature of intermetallics and an incremental undercooling for intermetallics pre-nucleation can be obtained. The nuclei can act as heterogeneous nucleation substrates for α-Al to facilitate grain refinement [26].
3) Cavitation can promote the wetting of nonwettable inclusions in the liquid melt (such as oxides) and turn them into potential heterogeneous nucleation sites [16].

As is shown in Fig. 2, UA-TRC achieved a desirable grain refinement without the addition of Al-5Ti-1B grain refiner. In the present study, ultrasonic treatment was conducted in the liquid state. Therefore, the dendrites fragment theory has lim-

Please cite this article in press as: Huang J, et al. Elimination of edge cracks and centerline segregation of twin-roll cast aluminum strip by ultrasonic melt treatment. J Mater Res Technol. 2020. https://doi.org/10.1016/j.jmrt.2020.03.021

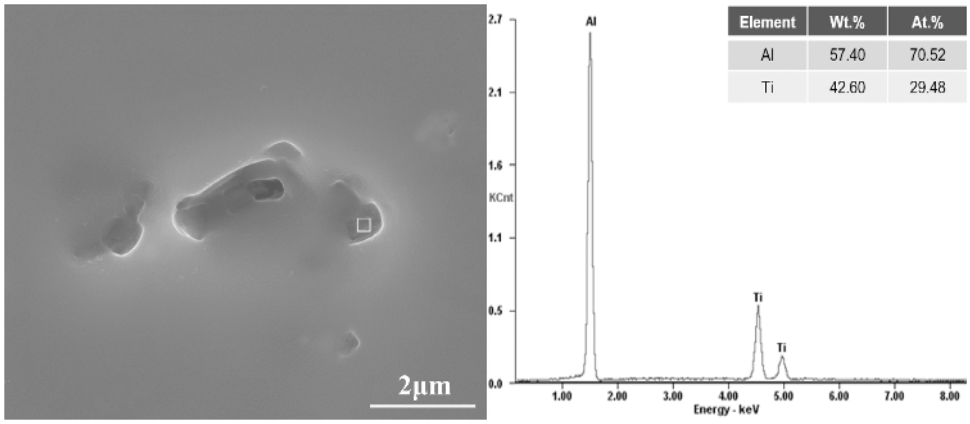

Fig. 10 – The Al_3Ti particles in the UA-TRC(Ti) strip, and the EDS result corresponding to white-square area.

Table 3 – Composition of TRC strips (in wt.%).

	Fe	Si	Ti	Cu	Mn	Mg	Al
Conventional TRC	0.29	0.065	0.019	<0.005	<0.005	<0.005	Bal.
UA-TRC(Ti)	0.28	0.067	0.026	<0.005	<0.005	<0.005	Bal.

ited contribution to the grain refinement. Commercial melts of aluminum alloys always contain many non-wettable particles, most of them are oxides [27]. Hence, heterogeneous nucleation theory is plausible according to the low lattice misfit between Al and Al_2O_3 particles [16], the latter of which unavoidably exist in liquid aluminum [28]. Nevertheless, it should be noted that the number of oxide particles in liquid melt is far less than the TiB_2 particles introduced by Al-5Ti-1B grain refiner. From this perspective, the heterogeneous nucleation based on inclusions might not be the primary mechanism of grain refinement in the current study. Dong et al. [18] and Komarov et al. [19] found that accompanied by corrosion of Ti and Nb sonotrode, thin layer of Al_3Ti particles and Al_3Nb were respectively formed and clung to the surface of titanium sonotrode and niobium sonotrode. Al_3Ti particles were also observed in the present study, as shown in Fig. 10. The composition of both conventional TRC strip and UA-TRC strip were shown in Table 3, after ultrasonic treatment, the content of Ti increased limitedly. Such Ti concentration is too low for precipitation of Al_3Ti (the peritectic point is at 0.15 wt.% Ti). From this perspective, it is proposed that the Al_3Ti particles were primarily formed upon the sonotrode surface and dispersed with acoustic flowing afterward. Accordingly, it is believed that the grain refinement in UA-TRC strip was relevant to heterogeneous nucleation on intermetallics. There is a theoretical approach to assess the potency of heterogeneous substrate, by calculating the lattice misfit at the interface between substrate and matrix along with a specific orientation relationship. The lattice misfit f is defined as the following formula:

$$f = \frac{\left|d[u\,v\,w]_{Al} - d[u'\,v'\,w']_S\right|}{d[u\,v\,w]_{Al}} \times 100\% \quad (2)$$

Where $d[u\,v\,w]_{Al}$ and $d[u'\,v'\,w']_S$ are the atomic spacing along the close-packed direction on the close-packed plane of the matrix and the substrate, respectively [28]. The relevant data are listed in Table 4. The misfit of either the interface of Al/Al_3Ti and Al/Al_3Nb were found to be far less than the suggested limit of 15% for potent lattice matching, which indicates that both Al_3Ti and Al_3Nb have stronger potency than the TiB_2 (4.22% in lattice misfit [29]) to become heterogeneous nucleation for the α-Al during solidification. The achievement of grain refinement by heterogeneous nucleation relies not only on the existence of potent substrates but also on adequate density as well as uniform distribution of such substrates. The latter two requirements can be realized by cavitation and acoustic streaming. Whilst the cavitation effect triggered the formation of appreciable substrates upon the sonotrode surface, the acoustic streaming helped in dispersing of the formed substrates throughout the melt volume [16]. As a corollary, the heterogeneous nucleation is promoted, resulting in grain refinement.

4.2. *Eliminating centerline segregation*

Iron (Fe) element has a high segregation tendency in liquid aluminum with a distribution coefficient of 0.03. As a result, during solidification in the conventional TRC, Fe element is expelled from solid to liquid which leads to the formation of Fe-rich areas [30]. Once the centerline segregation arose, large intermetallics would form at the central plane of the strip. The formation mechanism of centerline segregation is usually ascribed to inhomogeneous flow and pressure-induced channel segregation [31].

Grain refinement was suggested as an effective method to relieve segregation [32]. However, our results show an equivalent grain refinement in the conventional TRC and UA-TRC, while visible centerline segregation was still observed in the conventional TRC strip. It is reasonable to speculate that the enhanced flowing pattern when applying UA-TRC process is responsible for eliminating centerline segregation. Ultrasonic cavitation in aluminum melt has been observed by

Please cite this article in press as: Huang J, et al. Elimination of edge cracks and centerline segregation of twin-roll cast aluminum strip by ultrasonic melt treatment. J Mater Res Technol. 2020. https://doi.org/10.1016/j.jmrt.2020.03.021

Table 4 – Lattice parameters and lattice misfit f between Al matrix and potential substrates.

Interface	Structure & Lattice parameter/nm	Orientation relationship	f
Al/Al_3Ti	Al: FCC, a = 0.4049; Al_3Ti: Tetragonal, a = 0.3851; c = 0.8610	$(111)[110] \parallel (112)\left[20\bar{1}\right]$	0.87%
Al/Al_3Nb	Al: FCC, a = 0.4049;Al_3Nb: Tetragonal, a = 0.3840; c = 0.8580	$(111)[110] \parallel (112)\left[02\bar{1}\right]$	0.54%

synchrotron X-radiography recently, and the collapse of cavitation bubbles not only mechanically broke the dendrites by the high-speed micro-jets but also facilitated the acoustic flowing for opening up the dendrite network [33]. The initial velocity generated by micro-jets varies from 300 to 1000 m/s in terms of the different diameters of cavitation bubbles [34]. Such high-speed jets favor the shearing force and forced convection over the whole volume. In the case of conventional TRC process, the solute-rich liquid was eventually squeezed into the central plane since the liquid melt solidifies from the roll surface towards the center of strip. Once ultrasonic waves were introduced into molten aluminum, the enhanced convection could make the solute-rich liquid flow back to the liquid pool for further redistribution. Subsequently, the composition at the solidification interface became relatively homogeneous and the concentration of Fe elements at the center area was decreased. As a consequence, the centerline segregation was suppressed, as is shown in Figs. 4 and 5.

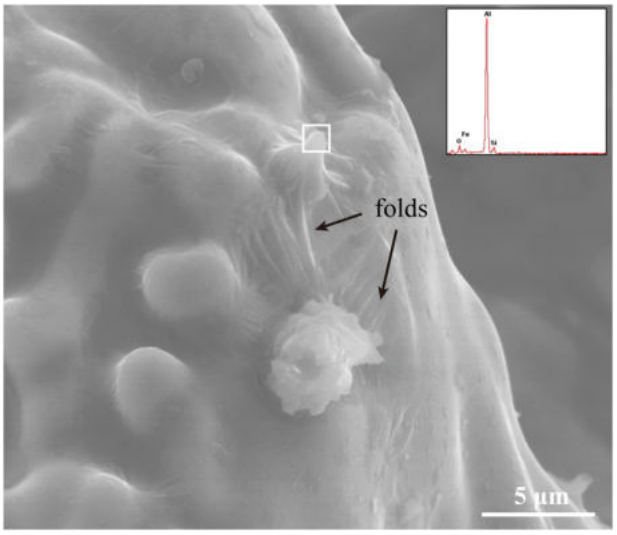

Fig. 11 – Feature of "liquid" film with folds on fracture surface. The inset is the EDS result corresponding to white-square area.

4.3. *Cause of edge cracks and its elimination regime*

The KAM maps show that the intergranular strain in the edge area of UA-TRC strip is a bit smaller than the conventional TRC one. According to KAM maps (Fig. 8(c) and (d)), the grains around the edge crack of the conventional TRC strip seem to present some local stress concentration. In UA-TRC process, owing to acoustic streaming, ultrasonic treatment provided a flat temperature gradient in the volume, which is responsible for the relaxation of thermal stresses. According to the criterion proposed by Campbell [35], thermal stresses generated during solidification shrinkage not only induced deformation but also pulled the dendrite arms apart. The cracks were formed if the permeability of the mushy zone was small and the separation of the dendrite cannot be compensated enough. Nonetheless, it should be noted that the difference of KAM values between the conventional TRC strip and UA-TRC strip is not exceedingly distinct, maybe within experimental scatter. Hence there is no apparent evidence that stress concentration is responsible for the edge crack.

Previous studies on the effect of grain size for hot-tearing susceptibility in aluminum alloys indicated that the fine grain size reduced hot-tearing effectively [36]. Fine grains can promote interdendritic feeding and low interlocking stresses. However, the grain refinement among all the trials in the present study was similar, which implies that the grain size is not a principal reason for the edge cracks, as shown in Figs. 2 and 8. As seen in Fig. 6, the dendrite morphology formed due to interdendritic solidification shrinkage and the remained liquid failed to feed during the TRC processing [20]. It is well known that the Fe-rich intermetallics increased porosity by blocking interdendritic feeding channels during solidification according to "restricted feeding" theory [21]. As solidification progressed, the liquid compensation gradually became more deficient, micro-pores occurred and interconnected, leading to the formation of macro-crack eventually. A close-up observation of dendrite arms of α-Al indicated a Fe-rich intermetallic covered by a "liquid" film with folds as is shown in Fig. 11. As the EDS result shows, the film contains oxygen element, revealing that the film was formed at a high temperature in the liquid/gas interface and its formation is accompanied by oxidation. This kind of oxide film impeded interdendritic feeding during solidification. Meanwhile, it is noticeable that the film wrinkled to some extent, as exhibited in Fig. 11. The appearances of folds indicate that the surrounding liquid failed to fill the gap among dendrites [37]. The liquid folds might be an indirect evidence of a little interdendritic solidification shrinkage that happened after the formation of the liquid film. Fig. 12 shows elemental mapping of the crack surface of the conventional TRC strip. The surface locates at edge area of the strip. Results suggested that Fe element enriched in the crack area and where slight oxidation occurred. In comparison, in the edge area of UA-TRC strip, as shown in Fig. 13, there was not evidence of Fe element segregation. Instead, Fe distributed fairly uniform. According to the striking difference of Fe element distribution between two strips, one of the reasons for the disappearance of edge cracks might on account of the uniformity of the Fe distribution. If Fe element segregates during solidification, coarse Fe-rich intermetallics would form which can impede the interdendritic feeding [21]. Upon application of US treatment, as discussed earlier, the acoustic streaming and micro-jets induced by ultrasonic treatment effectively improved the homogeneity

Please cite this article in press as: Huang J, et al. Elimination of edge cracks and centerline segregation of twin-roll cast aluminum strip by ultrasonic melt treatment. J Mater Res Technol. 2020. https://doi.org/10.1016/j.jmrt.2020.03.021

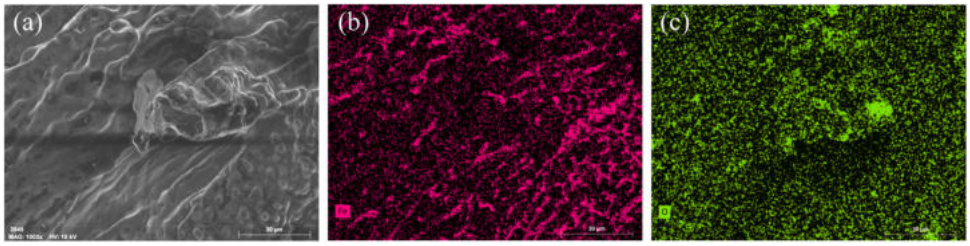

Fig. 12 – (a) The SE image of the crack surface corresponding to SEM-EDS elemental mappping of (b) iron and (c) oxygen.

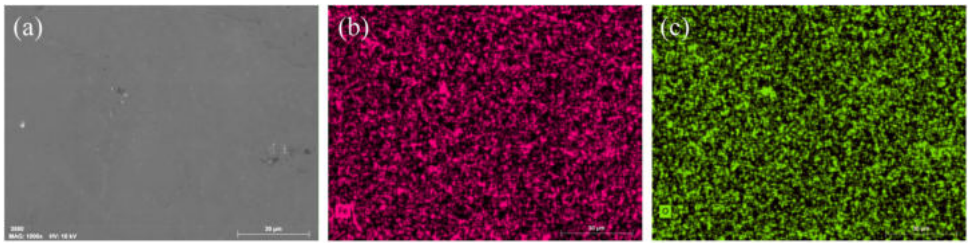

Fig. 13 – (a) The SE image of the edge area of UA-TRC strip and the elemental mappping of (b) iron and (c) oxygen.

of composition and liquid fluidity, which in turn increased the interdendritic feeding. Meanwhile, the permeability of the mushy zone increased due to additional heat and agitation introduced by cavitation, resulting in micro-cracks healing [38,39]. The disappearance of edge crack also benefits from such enhanced feeding.

5. Conclusions

In this study, ultrasonic melt treatment was conducted in TRC processing, as a comparison with the conventional TRC process. The conclusions can be summarized as below:

(1) The strip produced using the conventional TRC shows observable centerline segregation and clear macro edge cracks, even with Al-5Ti-1B grain refiner added. However, no visible cracks and segregation were found in UA-TRC strips.
(2) Edge cracks were formed in the conventional TRC strip due to inadequate feeding compensation, which was primarily caused by the non-uniformity distribution of Fe element at the edge regions. The coarse Fe-rich intermetallics and the "liquid" film impeded the interdendritic liquid feeding. With the combined action of cavitation and acoustic streaming, Fe element distributed uniformly and the interdendritic feeding was enhanced. As a consequence, the edge cracks were eliminated effectively.
(3) Owing to the acoustic streaming and micro-jets brought by ultrasonic, the liquid flowing in the sump was motivated, which further promoted the solute redistribution, and the centerline segregation was suppressed.
(4) Compared to the conventional TRC strip, the UA-TRC strips presented a desirable grain size without any addition of Al-5Ti-1B grain refiner. The grain refinement of UA-TRC could be attributed to the heterogeneous nucleation by Al_3Ti, Al_3Nb, and inclusions.
(5) Upon 5 h service time, less corrosion occurred on the niobium sonotrode despite the unavoidable dissolution of both sonotrode.

Conflicts of interest

The authors declare no conflicts of interest.

Acknowledgments

This work was supported by Tsinghua University Initiative Scientific Research Program (Grant No. 20173080030) and the International Science and Technology Cooperation Project of China (Grant No. 2015DFR50470).

REFERENCES

[1] Santos CA, Spim JA, Garcia A. Modeling of solidification in twin-roll strip casting. J Mater Process Technol 2000;102:33–9, http://dx.doi.org/10.1016/S0924-0136(00)00448-9.
[2] Zeng J, Koitzsch R, Pfeifer H, Friedrich B. Numerical simulation of the twin-roll casting process of magnesium alloy strip. J Mater Process Technol 2009;209:2321–8, http://dx.doi.org/10.1016/j.jmatprotec.2008.05.032.
[3] Kim MS, Kim HW, Kim SH, Kumai S. Role of roll separating force in high-speed twin-roll casting of aluminum alloys. Metals (Basel) 2019;9:3–9, http://dx.doi.org/10.3390/met9060645.
[4] Stjohn DH, Qian M, Easton MA, Cao P. The Interdependence Theory: the relationship between grain formation and nucleant selection. Acta Mater 2011;59:4907–21, http://dx.doi.org/10.1016/j.actamat.2011.04.035.
[5] Jin I, Morris LR, Hunt JD. Centerline segregation in twin-roll-cast aluminum alloy slab. JOM J Miner Met Mater Soc 1982;34:70–5, http://dx.doi.org/10.1007/BF03338033.

[6] Li BQ. Producing thin strips by twin-roll casting-part I: process aspects and quality issues. JOM 1995;47:29–33, http://dx.doi.org/10.1007/BF03221172.
[7] Lv Z, Du F, An Z, Huang H, Xu Z, Sun J. Centerline segregation mechanism of twin-roll cast A3003 strip. J Alloys Compd 2015;643:270–4, http://dx.doi.org/10.1016/j.jallcom.2015.04.132.
[8] Wang H, Zhou L, Zhang Y, Cai Y, Zhang J. Effects of twin-roll casting process parameters on the microstructure and sheet metal forming behavior of 7050 aluminum alloy. J Mater Process Technol 2016;233:186–91, http://dx.doi.org/10.1016/j.jmatprotec.2016.02.016.
[9] Gras C, Meredith M, Hunt JD. Microdefects formation during the twin-roll casting of Al-Mg-Mn aluminium alloys. J Mater Process Technol 2005;167:62–72, http://dx.doi.org/10.1016/j.jmatprotec.2004.09.084.
[10] Das S, Barekar N, El Fakir O, Yang X, Dear JP, Fan Z. Influence of intensive melt shearing on subsequent hot rolling and the mechanical properties of twin roll cast AZ31 strips. Mater Lett 2015;144:54–7, http://dx.doi.org/10.1016/j.matlet.2015.01.017.
[11] Barekar NS, Das S, Yang X, Huang Y, El Fakir O, Bhagurkar AG, et al. The impact of melt conditioning on microstructure, texture and ductility of twin roll cast aluminium alloy strips. Mater Sci Eng A 2016;650:365–73, http://dx.doi.org/10.1016/j.msea.2015.10.079.
[12] Kim K. The effect of melt conditioning on segregation of solute elements and nucleation of aluminum grains in a twin roll cast aluminum alloy. Metall Mater Trans A Phys Metall Mater Sci 2014;45:4538–48, http://dx.doi.org/10.1007/s11661-014-2414-y.
[13] Sun KM, Li L, Chen SD, Xu GM, Chen G, Misra RDK, et al. A new approach to control centerline macrosegregation in Al-Mg-Si alloys during twin roll continuous casting. Mater Lett 2017;190:205–8, http://dx.doi.org/10.1016/j.matlet.2016.12.109.
[14] Zhang D, Nastac L. Numerical modeling of the dispersion of ceramic nanoparticles during ultrasonic processing of aluminum-based nanocomposites. J Mater Res Technol 2014;3:296–302, http://dx.doi.org/10.1016/j.jmrt.2014.09.001.
[15] Fang Y, Yamamoto T, Komarov S. Cavitation and acoustic streaming generated by different sonotrode tips. Ultrason Sonochem 2018;48:79–87, http://dx.doi.org/10.1016/j.ultsonch.2018.05.011.
[16] Eskin GI, Eskin DG. Ultrasonic treatment of light alloy melts. CRC Press; 2014, http://dx.doi.org/10.1201/b17270.
[17] Wang M, Pang JC, Liu HQ, Li SX, Zhang ZF. Property optimization of low-cycle fatigue in Al-Si piston alloy at elevated temperatures by ultrasonic melt treatment. J Mater Res Technol 2019;8:4556–68, http://dx.doi.org/10.1016/j.jmrt.2019.07.069.
[18] Dong F, Li X, Zhang L, Ma L, Li R. Cavitation erosion mechanism of titanium alloy radiation rods in aluminum melt. Ultrason Sonochem 2016;31:150–6, http://dx.doi.org/10.1016/j.ultsonch.2015.12.009.
[19] Komarov S, Kuznetsov D. Erosion resistance and performance characteristics of niobium ultrasonic sonotrodes in molten aluminum. Int J Refract Met Hard Mater 2012;35:76–83, http://dx.doi.org/10.1016/j.ijrmhm.2012.04.004.
[20] Kim MS, Arai Y, Hon Y, Kumai S. Formation of internai crack in high-speed twin-roll cast 6022 aluminum alloy strip. Mater Trans 2010;51:1854–60, http://dx.doi.org/10.2320/matertrans.L-M2010818.
[21] Zhang L, Gao J, Damoah LNW, Robertson DG. Removal of iron from aluminum: a review. Miner Process Extr Metall Rev 2012;33:99–157, http://dx.doi.org/10.1080/08827508.2010.542211.
[22] Otarawanna S, Gourlay CM, Laukli HI, Dahle AK. Agglomeration and bending of equiaxed crystals during solidification of hypoeutectic Al and Mg alloys. Acta Mater 2010;58:261–71, http://dx.doi.org/10.1016/j.actamat.2009.09.002.
[23] Qian M, Ramirez A, Das A. Ultrasonic refinement of magnesium by cavitation: clarifying the role of wall crystals. J Cryst Growth 2009;311:3715, http://dx.doi.org/10.1016/j.jcrysgro.2009.04.036.
[24] Tzanakis I, Lebon GSB, Eskin DG, Pericleous KA. Characterizing the cavitation development and acoustic spectrum in various liquids. Ultrason Sonochem 2017;34:651–62, http://dx.doi.org/10.1016/j.ultsonch.2016.06.034.
[25] Swallowe GM, Field JE, Rees CS, Duckworth A. A photographic study of the effect of ultrasound on solidification. Acta Metall 1989;37:961–7, http://dx.doi.org/10.1016/0001-6160(89)90023-0.
[26] Huang H, Shu D, Zeng J, Bian F, Fu Y, Wang J, et al. In situ small angle X-ray scattering investigation of ultrasound induced nucleation in a metallic alloy melt. Scr Mater 2015;106:21–5, http://dx.doi.org/10.1016/j.scriptamat.2015.04.011.
[27] Li C, guo Li J, zhe Mao Y, cheng Ji J. Mechanism to remove oxide inclusions from molten aluminum by solid fluxes refining method. China Foundry 2017;14:233–43, http://dx.doi.org/10.1007/s41230-017-7005-2.
[28] Wang Y, Li HT, Fan Z. Oxidation of aluminium alloy melts and inoculation by oxide particles. Trans Indian Inst Met 2012;65:653–61, http://dx.doi.org/10.1007/s12666-012-0194-x.
[29] Fan Z, Wang Y, Zhang Y, Qin T, Zhou XR, Thompson GE, et al. Grain refining mechanism in the Al/Al-Ti-B system. Acta Mater 2015;84:292–304, http://dx.doi.org/10.1016/j.actamat.2014.10.055.
[30] Du Q, Eskin DG, Katgerman L. Modeling macrosegregation during direct-chill casting of multicomponent aluminum alloys. Metall Mater Trans A Phys Metall Mater Sci 2007;38:180–9, http://dx.doi.org/10.1007/s11661-006-9042-0.
[31] Kim MS, Kim SH, Kim HW. Deformation-induced center segregation in twin-roll cast high-Mg Al–Mg strips. Scr Mater 2018;152:69–73, http://dx.doi.org/10.1016/j.scriptamat.2018.04.017.
[32] Westengen H, Nes K. Twin roll casting of aluminium: The occurrence of structure inhomogeneities and defects in as cast strip. Essent Readings Light Met 2013;3:972–80, http://dx.doi.org/10.1002/9781118647783.ch123.
[33] Wang F, Eskin D, Mi J, Wang C, Koe B, King A, et al. A synchrotron X-radiography study of the fragmentation and refinement of primary intermetallic particles in an Al-35 Cu alloy induced by ultrasonic melt processing. Acta Mater 2017;141:142–53, http://dx.doi.org/10.1016/j.actamat.2017.09.010.
[34] Tzanakis I, Eskin DG, Georgoulas A, Fytanidis DK. Incubation pit analysis and calculation of the hydrodynamic impact pressure from the implosion of an acoustic cavitation bubble. Ultrason Sonochem 2014;21:866–78, http://dx.doi.org/10.1016/j.ultsonch.2013.10.003.
[35] Campbell J. Castings. Elsevier Ltd.; 2003, http://dx.doi.org/10.1016/B978-0-7506-4790-8.X5016-5.
[36] Lin S, Aliravci C, Pekguleryuz MO. Hot-tear susceptibility of aluminum wrought alloys and the effect of grain refining. Metall Mater Trans A Phys Metall Mater Sci 2007;38:1056–68, http://dx.doi.org/10.1007/s11661-007-9132-7.

Please cite this article in press as: Huang J, et al. Elimination of edge cracks and centerline segregation of twin-roll cast aluminum strip by ultrasonic melt treatment. J Mater Res Technol. 2020. https://doi.org/10.1016/j.jmrt.2020.03.021

[37] Xu R, Zheng H, Luo J, Ding S, Zhang S, Tian X. Role of tensile forces in hot tearing formation of cast Al – Si alloy. Trans Nonferrous Met Soc China 2014;24:2203–7, http://dx.doi.org/10.1016/S1003-6326(14)63333-1.
[38] Pilling J, Hellawell A. Mechanical deformation of dendrites by fluid flow. Metall Mater Trans A Phys Metall Mater Sci 1996;27:229–32, http://dx.doi.org/10.1007/BF02647763.
[39] Réger M, Verö B, Józsa R, Csepeli Z. Effect of mushy zone permeability on the formation of centerline segregation in slab casting. Mater Sci Forum 2014;790–391:296–301, http://dx.doi.org/10.4028/www.scientific.net/MSF.790-791.296.

Please cite this article in press as: Huang J, et al. Elimination of edge cracks and centerline segregation of twin-roll cast aluminum strip by ultrasonic melt treatment. J Mater Res Technol. 2020. https://doi.org/10.1016/j.jmrt.2020.03.021